TISSUE ENGINEERING: Part A
Volume 00, Number 00, 2014

DOI: 10.1089/ten.tea.2013.0741

Original Article

Magnesium-Containing Nanostructured Hybrid Scaffolds for Enhanced Dentin Regeneration

Tiejun Qu, DDS, PhD,[1,2] Junjun Jing, PhD,[1,3] Yong Jiang, DDS, PhD,[1,2] Robert J. Taylor, PhD,[4] Jian Q. Feng, MD, PhD,[1] Benjamin Geiger, PhD,[5] and Xiaohua Liu, PhD[1]

Dental caries is one of the most prevalent chronic diseases in the United States, affecting 92% of adults aged 20–64 years. Scaffold-based tissue engineering represents a promising strategy to replace damaged dental structures and restore their biological functions. Current single-component scaffolding materials used for dental tissue regeneration, however, cannot provide the proper microenvironment for dental stem/progenitor cell adhesion, proliferation, and differentiation; new biomimetic hybrid scaffolds are needed to promote better dental tissue formation. In this work, we developed a biomimetic approach to prepare three-dimensional (3D) nanofibrous gelatin/magnesium phosphate (NF-gelatin/MgP) hybrid scaffolds. These scaffolds not only mimic the nanostructured architecture and the chemical composition of natural dentin matrices but also constantly present favorable chemical signals (Mg ions) to dental pulp stem cells (DPSCs), thus providing a desirable microenvironment to facilitate DPSC proliferation, differentiation, and biomineralization. Synthesized hybrid NF-gelatin/MgP possesses natural extracellular matrix (ECM)-like architecture, high porosity, high pore interconnectivity, well-defined pore size, and controlled Mg ion release from the scaffold. Adding MgP into NF-gelatin also increased the mechanical strength of the hybrid scaffold. The sustained release of Mg ions from the NF-gelatin/MgP (MgP = 10% wt/wt) scaffold significantly enhanced the proliferation, differentiation, and biomineralization of human DPSCs *in vitro*. The alkaline phosphatase (ALP) activity and the gene expressions for odontogenic differentiation (collagen I [*Col I*], *ALP*, osteocalcin [*OCN*], dentin sialophosphoprotein [*DSPP*], and dentin matrix protein 1 [*DMP1*]) were all significantly higher ($p < 0.05$) in the NF-gelatin/MgP group than in the NF-gelatin group. Those results were further confirmed by hematoxylin and eosin (H&E) and von Kossa staining, as shown by greater ECM secretion and mineral deposition in the hybrid scaffold. Consistent with the *in vitro* study, the DPSCs/NF-gelatin/MgP constructs produced greater ECM deposition, hard tissue formation, and expression of marker proteins (DSPP, DMP1, Col I) for odontogenic differentiation than did the DPSCs/NF-gelatin after 5 weeks of ectopic implantation in rude mice. The controlled release of metallic ions from biomimetic nanostructured hybrid scaffolds, therefore, is a promising approach to enhancing the biological capability of the scaffolds for dental tissue regeneration.

Introduction

Dental caries is one of the most prevalent chronic diseases of all populations worldwide.[1] According to the report from the National Institute of Dental and Craniofacial Research (NIDCR), 92% of adults aged 20–64 years in the United States have had dental caries in their permanent teeth.[2] Clinically, if caries progresses and inflames pulp tissues inside the tooth, a root canal procedure (the most widely used method in endodontics) must be performed to remove the necrotic dental tissues, clean the pulp chamber, and seal it with bioinert materials (e.g., gutta percha). While this therapy has been used for many years, the tooth repair it offers is nonbiological and has several limitations, including unpleasant sensations, poor biocompatibility, damage to surrounding tissues, and unpredictable long-term therapeutic efficiency.[3,4] It has also been shown that endodontically treated teeth tend to become brittle and susceptible to postoperative fracture.[5] Therefore, the development of an alternative to traditional root canal treatment has long been a clinical goal of regenerative endodontics.

The regeneration of dental tissues using a scaffold-based tissue engineering strategy represents a promising approach

[1]Department of Biomedical Sciences, Texas A&M University Baylor College of Dentistry, Dallas, Texas.
[2]State Key Laboratory of Military Stomatology, Department of Operative Dentistry and Endodontics, School of Stomatology, Fourth Military Medical University, Xi'an, China.
[3]State Key Laboratory of Oral Diseases, West China Hospital of Stomatology, Sichuan University, Chengdu, China.
[4]Department of Veterinary Integrative Biosciences (VIBS), Texas A&M University College of Veterinary Medicine, College Station, Texas.
[5]Department of Molecular Cell Biology, The Weizmann Institute of Science, Rehovot, Israel.

to replace damaged dentin/pulp structures and restore their biological functions.[6–9] A scaffold is an artificial extracellular matrix (ECM) and serves as a temporal template for tissue regeneration. Ideally, a scaffold should be biodegradable, biocompatible, promote cellular interactions and tissue development, and possess proper mechanical properties.[10–14] In an attempt to regenerate dentin and pulp, several types of scaffolds, including collagen, poly(lactide-co-glycolide), synthetic peptides, and porous ceramic, have been tested with dental pulp stem cells (DPSCs) both *in vitro* and *in vivo*.[7,15–18] However, all of those studies regenerated only limited dental tissues randomly distributed inside the scaffolding constructs, indicating that single-component scaffolding materials cannot provide the proper microenvironment for DPSC adhesion, proliferation, and differentiation. Thus, new biomimetic hybrid scaffolds are needed for better dental tissue regeneration.

Magnesium (Mg) is the fourth most abundant cation in the body; the average Mg concentration in dentin is about 1% (wt/wt).[19] Mg affects many cellular functions, including the modulation of signal transduction, energy metabolism, cell proliferation, and differentiation.[19–22] Mg is also associated with the biomineralization of bone and tooth[19] and indirectly influences mineral metabolism, for example, through the activation of alkaline phosphate (ALP).[20] In addition, Mg directly affects the crystallization processes and pattern formation of the inorganic mineral phase.[23] Magnesium phosphate (MgP) cement has been shown to promote the proliferation and differentiation of human bone marrow stem cells.[24–26] Mg ions have also been implanted to titanium surfaces to enhance bone formation.[27] However, to date, the exploration of Mg-containing biomaterials for dental tissue regeneration has not been attempted.

In this study, we incorporated MgP into three-dimensional (3D) nanofibrous gelatin (NF-gelatin) matrices to form a novel hybrid scaffold for enhanced dentin regeneration. NF-gelatin matrix was prepared to mimic both the chemical composition and physical architecture of natural collagen (type I), which is the main organic component of the dentin matrix. The 3D NF-gelatin possessed abundant porosities ($>96\%$), a large surface area ($>32\,m^2/g$), good mechanical properties (compressive modulus 300–800 kPa), and nanofibrous pore wall structures (average fiber diameter approximate 160 nm).[28] The *in vitro* results further showed that the NF-gelatin scaffold provided better microenvironments for cell adhesion, proliferation, and differentiation than conventional gelatin counterparts.[28] MgP was incorporated into the NF-gelatin during the solvent casting and thermally induced phase separation (TIPS) process. We hypothesized that the sustained release of Mg ions from the MgP in the hybrid scaffold would significantly enhance the proliferation and odontogenic differentiation of human DPSCs in the scaffold. For this purpose, we first examined the effect of the Mg ion concentration on human DPSCs in a 2D culture plate system. The adhesion, proliferation, differentiation, and biomineralization of human DPSCs on the 3D hybrid scaffold and the control group (NF-gelatin only) were then examined both *in vitro* and *in vivo*. Our results showed that NF-gelatin supports human DPSC growth, and the incorporation of the MgP into the biomimetic scaffold significantly enhanced the odontogenic differentiation of human DPSCs *in vitro* and formed much more dentin-like tissue *in vivo*.

Materials and Methods

Materials

Gelatin was purchased from Sigma-Aldrich; N-hydroxysuccinimide (97%) (NHS) and 2-(N-morpholino) ethanesulfonic acid) hydrate (MES) were purchased from Aldrich Chemical; and 1-ethyl-3-(3-dimethylaminopropyl) carbodiimide HCl (EDC) was purchased from Pierce Biotechnology. Calcium dihydrogen phosphate, magnesium oxide, and all other reagents were obtained from Thermo Fisher Scientific.

DPSCs cultured on 2D plates with the addition of Mg ions

The human DPSCs used in this study were a gift from Dr. Songtao Shi, School of Dentistry, University of Southern California. The thawed DPSCs (passage 2) were cultured in ascorbic acid-free α-modified essential medium (α-MEM) (Gibco, Invitrogen) supplemented with 10% fetal bovine serum (FBS) (Invitrogen) and 1% penicillin–streptomycin (Invitrogen) in a humidified incubator with 5% CO_2 at 37°C. The culture medium was changed every 2 days. The DPSCs of passages 4–6 were used for all cellular studies.

A total of 5×10^3 DPSCs were seeded into each well of a 24-well plate and cultured in α-MEM supplemented with 10% FBS at 37°C. The culture medium was changed every other day. For the differentiation experiment after the cells proliferated to 80% confluence, the DPSCs were cultured in the odontogenic medium (containing 50 μg/mL ascorbic acid, 5 mM β-glycerophosphate, and 10 nM dexamethasone) with the addition of 0, 100, 500, or 1000 ppm $MgCl_2$ in the culture medium.

Measurements of the proliferation and differentiation of DPSCs on 2D plates

The proliferation of the human DPSCs on 2D culture plates was determined by the 3-(4, 5-dimethylthiazol-2-yl)-2, 5-diphenyl-2, 5-tetrazoliumbromide (MTT) assay. The DPSCs were seeded into 96-well plates at a density of 2×10^3 cells per well and kept for 24 h, starved in serum-free media for another 24 h and then treated with $MgCl_2$-conditioned media at different concentrations (0, 100, 500, and 1000 ppm). At 1, 3, and 7 days after the $MgCl_2$ treatment, 20 μL fresh MTT solution (5 mg/mL; Sigma-Aldrich) was added to the wells of each group and incubated at 37°C for 4 h. The culture media were subsequently removed, and formazan was solubilized in 150 μL per well of dimethyl sulfoxide (Sigma); the absorbance (OD value) was measured at a wavelength of 570 nm. The data were described as the mean ± SD ($n=6$), and the experiment was repeated three times.

To evaluate the odontoblastic gene expression after treatment with the different concentrations of $MgCl_2$ for 3 weeks, the total cellular RNA was extracted by RNeasy Plus MiniKit (Qiagen) according to the manufacturer's instructions. The mRNA was reversed using QuantiTect Rev. Transcription Kit (Qiagen). Real-time reverse transcription-polymerase chain reaction (RT-PCR) was performed using a power SYBR Green QPCR Master Mix (Applied Biosystems) and the Bio-Rad Real-Time PCR Detection System (Bio-Rad). The reactions were repeated three times.

To evaluate odontogenesis, the human DPSCs were stained with Alizarin red (Sigma-Aldrich) on day 28. Each group was fixed using 4% paraformaldehyde (PFA), washed with distilled water, and stained with 2% Alizarin red for 10 min at room temperature. The specimens were then washed several times with distilled water to remove unspecific Alizarin red staining. Phosphate-buffered saline (PBS) was added to the samples, and images were obtained using a photo scanner (Epson).

Preparation of 3D nanostructured hybrid scaffolds

Three-dimensional nanostructured hybrid scaffolds were fabricated by combining a solvent cast, TIPS, and the porogen leaching process. Calcium dihydrogen phosphate was mixed with magnesium oxide at a molar ratio of 1:2 to form MgP.[29] A gelatin solution was prepared separately by dissolving 1 g gelatin in 10 mL water/ethanol (50/50, v/v) mixture at 50°C for 1h. Subsequently, a predetermined amount of MgP was added to the gelatin solution, which was stirred at 50°C for another 2 h to form a uniform solution. The solution (0.2 mL) was then cast onto paraffin-sphere assemblies prepared as described previously.[12] The gelatin-MgP solution in the paraffin assembly was phase-separated at −80°C for 12 h. Next, the gelatin-MgP-paraffin sphere assembly composites were immersed three times in 20 mL 1,4-dioxane for solvent exchange (fresh 1,4-dioxane was replaced every 8 h) and freeze-dried for 3 days. The composites were cut into 1.5 mm slices and then soaked in 50 mL hexane to leach out the paraffin spheres. The hexane was changed six times every 12 h to remove any residual paraffin in the scaffold. Then, cyclohexane (10 mL) was used to exchange the hexane in the scaffold for 4 h. Finally, the hybrid scaffold was freeze-dried for 24 h. For comparison, an NF-gelatin control sample was prepared using the same method, except that no MgP was added to the gelatin solution.

Because the gelation temperature of gelatin (approximate 32°C) is below the cell culture temperature (37°C), the NF-gelatin-MgP hybrid scaffold must be crosslinked to improve its thermal and mechanical stabilities before using it for tissue engineering purposes. Chemical crosslinking of the hybrid scaffolds with EDC and NHS was carried out in the MES buffer (pH 5.3, 0.05 M) at 4°C. To maintain the microstructure and prevent the swelling of the gelatin matrices in water, acetone/water (90/10, v/v) solvent mixture was chosen instead of pure water. After crosslinking for the designated times, the reaction was stopped by adding 0.1 M glycine, and the scaffolds were washed three times with distilled water at 37°C and freeze-dried for 24 h and stored in a desiccator for later use.

Characterization of the 3D nanostructured hybrid scaffolds

Surface morphology examination, Mg elemental analysis, and porosity calculation. The surface morphology of the scaffolds was examined using a scanning electron microscope (SEM; JEOL JSM-6010LA) with an accelerating voltage of 10 kV. The porosity of the scaffold was calculated as we reported previously.[28] The elemental contents and their distribution on the surface of the scaffolds were measured with the energy dispersive X-ray spectroscopy (EDS) associated with the SEM. The scaffolds were gold-coated for 120 s using a sputter coater (SPI-Module Sputter Coater Unit; SPI Supplies/Structure Probe, Inc.). During the process of gold coating, the gas pressure was set at 50 mTorr, and the current was 20 mA.

Attenuated total reflection–Fourier transform infrared (ATR-FTIR) spectroscopy. The attenuated total reflection-Fourier transform infrared (ATR-FTIR) spectra of NF-gelatin/MgP were obtained with a Nicolet iS10 FTIR spectrometer (Thermo Fisher Scientific). A range of 500–4000 cm^{-1} was scanned at a resolution of 1 cm^{-1}, and the signals were averaged.

Mechanical test. The compressive moduli of the scaffolds were measured using a mechanical tester (TestResources) as reported previously.[13,28] All the specimens were circular discs (17 mm in diameter and 1.5 mm in thickness); they were compressed at a crosshead speed of 0.5 mm/min, and the stress versus strain curve was recorded. The modulus was calculated as the slope of the linear portion of the stress–strain curve, and the averages and standard deviations were reported ($n = 3$).

In vitro release of Mg ions from hybrid scaffolds. The NF-gelatin-MgP hybrid scaffolds (diameter = 5 mm, thickness = 1.5 mm) were immersed in 1 mL phosphate Tris buffer at pH = 7.4 and incubated at 37°C, as we described previously.[30] At designated time points (1, 3, 7, 14, and 21 days), the samples were centrifuged to collect the supernatant, which was replaced with equal amounts of Tris buffer. The release of Mg ions from the NF-gelatin-MgP hybrid scaffold was determined with an inductively coupled plasma optical emission spectrometer (ICP-OES; Thermo Scientific).

DPSC seeding onto 3D biomimetic scaffolds

The scaffolds (NF-gelatin-MgP and NF-gelatin) were soaked in 70% ethanol for 30 min, and a low vacuum (~30 Torr) was added to remove air bubbles in them. They were washed three times (30 min each) with PBS to remove the residual ethanol. After that, the scaffolds were washed twice with α-MEM containing 10% FBS (2 h each). Human DPSCs (5×10^5) were then seeded onto each scaffold. The cell-scaffold constructs were cultured in α-MEM supplemented with 10% FBS for 24 h before being transferred to 12-well plates containing 2 mL medium in each well. For the differentiation of DPSCs, the ''odontogenic'' medium (made up of 50 μg/mL ascorbic acid, 5 mM β-glycerophosphate, and 10 nM dexamethasone) was used. All the cell–scaffold constructs were cultured at 37°C on an orbital shaker (OrbishakerTMCO_2; Benchmark) in an incubator with 5% CO_2. The culture medium was changed every other day.

Characterization of DPSCs seeded on 3D biomimetic scaffolds

DNA assay. To determine the proliferation of human DPSCs on the 3D scaffolds, the cell–scaffold constructs were homogenized in 1 mL 1× DNA assay buffer (Sigma) using an ultrasonic homogenizer (Virsonic60; Virtis). One milliliter of cell lysis buffer was added, and the samples were incubated at 37°C for 1 h. The cell lysis was spun

down at 5000 g for 5 min. The total DNA was quantified using a fluorescence assay (QuantiFluor™; Promega) with Hoechst 33258 dye according to the manual (Sigma).

SEM observation. The cell–scaffold constructs harvested after 3 weeks were rinsed in PBS followed by fixation in 2.5% glutaraldehyde for 24 h, then postfixed in 1% osmium tetroxide for 1 h. The specimens were subsequently dehydrated in a series of increasing concentrations of ethanol and hexamethyldisilazane and sputter-coated with gold and observed under an SEM (JEOL JSM-6010LA) at 10 kV.

ALP activity quantification. ALP activity was detected using a SensoLyte™ pNPP ALP Assay Kit (AnaSpec) according to the manufacturer's protocol. Briefly, the cells on the scaffold were homogenized in 1 mL of the lysis buffer supplied with the kit. The lyses were centrifuged at 10,000 g and 4°C for 15 min. The supernatant was collected for ALP assay using p-nitrophenyl phosphate as a phosphatase substrate and the ALP supplied by the kit as a standard. The absorbance was measured at 405 nm, and the amount of ALP in the cells was normalized against total protein content.

Hematoxylin and eosin staining and von Kossa staining. After 5 weeks of culture, the cell–scaffold constructs were fixed in 4% PFA at 4°C for 1 h. The samples were sequentially washed under water, dehydrated in ethanol, cleared in xylene, and embedded in paraffin. The specimens were then cut laterally into alternating 5-μm-thick sections and stained with hematoxylin and eosin (H&E) for histological examination. In the von Kossa staining procedure, the specimens were rinsed with PBS and fixed with 4% PFA. A von Kossa method for calcium kit (Polysciences) was used to stain the calcium deposits according to the protocol provided by the manufacturer. Quantitative analyses were performed using the ImageJ software as described by Nair *et al.*[31]

RT-PCR. The total RNA was extracted using Trizol (Invitrogen), and the first-strand cDNA was reverse-transcribed with TaqMan reverse transcription reagents (Applied Biosystems) from each sample. Human-specific primers were designed and synthesized as follows[32]: collagen α(1) I (sense 5′-AAAAGGAAGCTTGGTCCACT-3′; antisense 5′-GTGTG GAGAAAGGAGCAGAA-3′), ALP (sense 5′-CCACGTCTT CACATTTGGTG-3′; antisense 5′-AGACTGCGCCTGGTA GTTGT-3′), dentin matrix protein 1 (DMP1; sense 5′-TGGG GATTATCCTGTGCTCT-3′; antisense 5′-TACTTCTGGG GTCACTGTCG-3′), osteocalcin (OCN; sense 5′-ACTGTGA CGAGTTGGCTGAC-3′; antisense 5′-CAAGGGCAAGAGG AAAGAAG-3′), and dentin sialophosphoprotein (DSPP; sense 5′-TTAAATGCCAGTGGAACCAT-3′, antisense 5′-AT TCCCTTCTCCCTTGTGAC-3′). Glyceraldehyde-3-phosphate dehydrogenase (sense 5′-GAGTCAACGGATTTGGTCGT-3′; antisense 5′-GACAAGCTTCCCGTTCTGAG-3′) and GAPDH (sense 5′-AGCCGCATCTTCTTTTGCGTC-3′; antisense 5′-TCATATTTGGCAGGTTTTTCT-3′) was used as an internal control. The conditions for real-time PCR were as follows: denaturation at 95°C (10 min); 45 cycles at 95°C (15 s), 55°C (1 min, annealing) followed by a final dissociation step. The qRT-PCRs were performed using power SYBR Green QPCR Master Mix (Applied Biosystems) and the Bio-Rad Real-Time PCR Detection System (Bio-Rad). The reactions were measured three times.

In vivo subcutaneous implantation

The animal surgical procedure was approved by the University Committee on Use and Care of Animals (UCUCA) of the Texas A&M University Baylor College of Dentistry. Immunocompromised nude mice (nu/nu, 6 weeks; Charles River Laboratories) were used for the implantation. All the animals were anesthetized by intramuscular injection of xylazine/ketamine. The back of each animal was washed and disinfected with povidoneiodine. One midsagittal incision was made on the dorsa, and two subcutaneous pockets were created using blunt dissection. Cell–scaffold constructs with tooth slices were induced in the odontogenic medium for 2 weeks before subcutaneous implantation. Four specimens were implanted for each group, in which each mouse received two implants at random. After scaffold placement, the incisions were closed with suture. The animals were sacrificed and the specimens retrieved after 5 weeks of transplantation. The harvested specimens were immediately fixed in 10% (w/v) formalin for 24 h. All the specimens were observed by X-Ray (Faxitron MX-20DC12). After decalcification in EDTA for 5 weeks, the samples were processed for histological observation by H&E staining. For immunohistochemical analysis, 5-μm-thick paraffin-embedded sections were deparaffinized using xylene and ethanol and then immersed in primary human Collagen I (Col I), DMP1, and DSPP antibody (1:100 dilution) (Abcam). The immunohistochemical staining experiments were carried out using an ABC kit and a DAB kit (Vector Laboratories).

Statistical analysis

The data were reported as means ± standard deviations ($n = 3$). Statistical analysis was carried out using a Student's t-test for the differences among the groups. A value of $p < 0.05$ was considered to be statistically significant.

Results

DPSCs cultured on 2D plates with different Mg ion concentrations

We first examined the effect of Mg ions on DPSC proliferation, differentiation, and biomineralization on a 2D cell culture plate. As shown in Figure 1A, the proliferation rate of the DPSCs in the culture medium with 100 ppm Mg ions was higher than for the control group. As the Mg ion concentration increased to 500 and 1000 ppm, the growth rate of the DPSCs was slower than that of the control group, indicating that only a low Mg ion concentration benefitted DPSC proliferation. However, all three Mg ion concentrations significantly enhanced the odontogenic differentiation of the DPSCs (Fig. 1B). Alizarin red staining further indicated that the biomineralization of the DPSCs increased with the addition of Mg ions to the culture medium (Fig. 1C). Overall, the DPSCs had increased proliferation, differentiation, and biomineralization rates only at the Mg ion concentration of 100 ppm. Therefore, this concentration of Mg ions was used for our NF-gelatin/MgP hybrid scaffolding design, fabrication, and consequently, the cellular experiments.

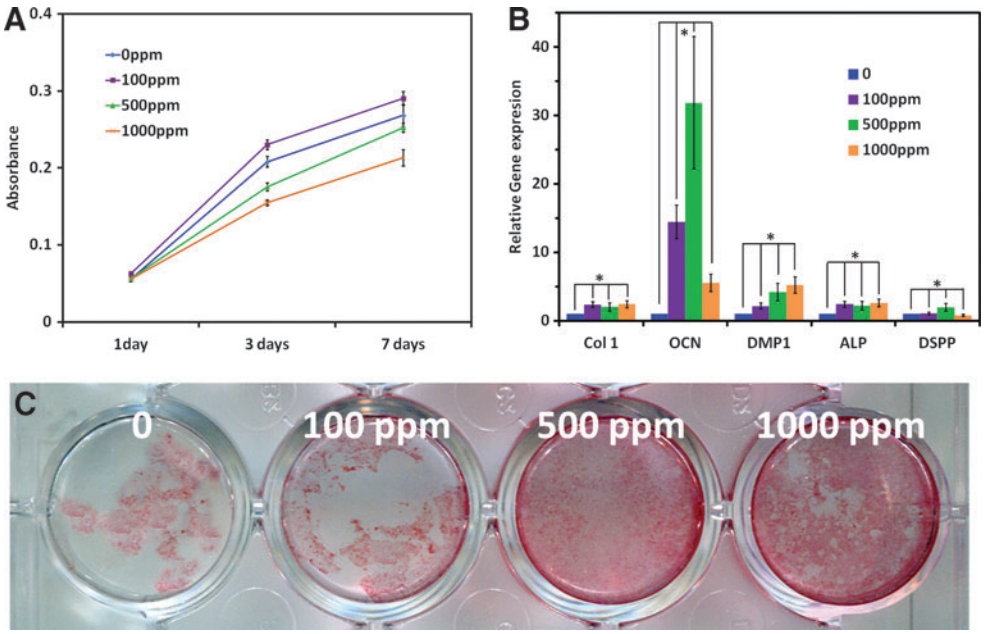

FIG. 1. Effects of adding Mg ions in the culture medium of 2D culture plates on the proliferation, differentiation, and biomineralization of dental pulp stem cells (DPSCs). **(A)** MTT assay showed that adding 100 ppm Mg ions increased DPSC proliferation compared to the control group from 1 to 7 days. However, the DPSCs had lower proliferation rates when high concentrations of Mg ions (500 and 1000 ppm) were added to the culture medium. **(B)** Relative gene expression (collagen type I [*Col I*], osteocalcin [*OCN*], dentin matrix protein 1 [*DMP1*], alkaline phosphatase (*ALP*), and dentin sialophosphoprotein [*DSPP*]) after human DPSCs were cultured on a 12-well plate for 3 weeks (*$p < 0.05$ between the Mg ions treated and the control groups). **(C)** Alizarin red staining revealed that the DPSCs treated by 100, 500, and 1000 ppm Mg ions conditioned media displayed more mineralized nodules than the control group after 4 weeks of culturing. Color images available online at www.liebertpub.com/tea

Characterization of the hybrid scaffolds

The NF-gelatin/MgP hybrid scaffolds were prepared by a process involving TIPS and porogen leaching steps. As shown in Figure 2, the hybrid scaffolds had a porous structure (porosity 96.5% ± 0.2%) with macropores ranging from 250 to 420 μm, which were controlled by the size of the paraffin sphere templates and were considered to be the optimal sizes for osteoblastic and odontoblastic cell adhesion, proliferation, and differentiation.[10] The incorporation of a small amount of MgP (10% wt in the scaffold) into the NF-gelatin did not affect the macropore size or the porosity of the hybrid scaffold. Each macropore of the scaffold was interconnected to other pores in the scaffold, and the pore walls were composed of gelatin nanofibers (Fig. 2B, E). Higher magnification further indicated that these nanofibers were between 50 and

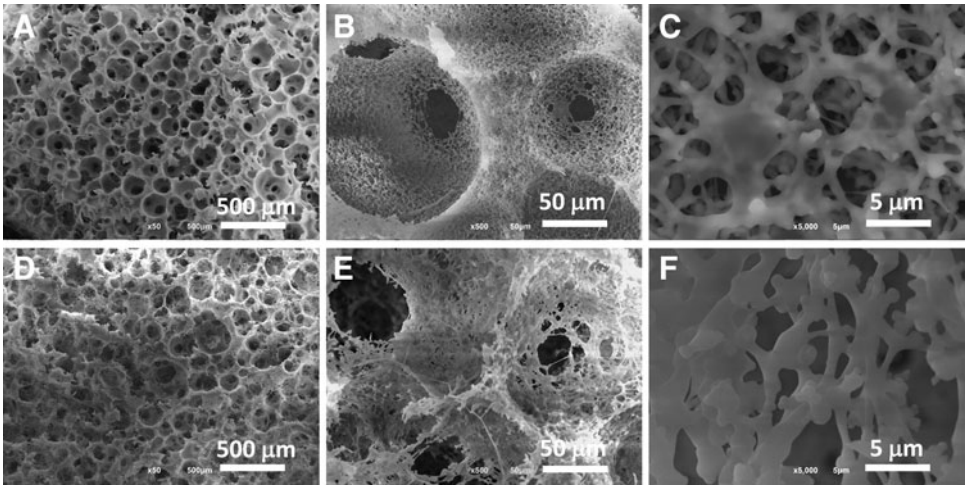

FIG. 2. Scanning electron microscope (SEM) micrographs of nanofibrous (NF)-gelatin and NF-gelatin/magnesium phosphate (MgP) hybrid scaffolds. **(A)** NF-gelatin scaffold, overview. **(B)** High magnification of **(A)** showing pore wall morphology of the NF-gelatin scaffold. **(C)** High magnification of **(B)** showing gelatin nanofibers of the NF-gelatin scaffold. **(D)** NF-gelatin/MgP (MgP = 10% wt/wt) scaffold overview. **(E)** High magnification of **(D)** showing pore wall morphology of the NF-gelatin/MgP scaffold. **(F)** High magnification of **(E)** showing gelatin nanofibers of the NF-gelatin/MgP scaffold.

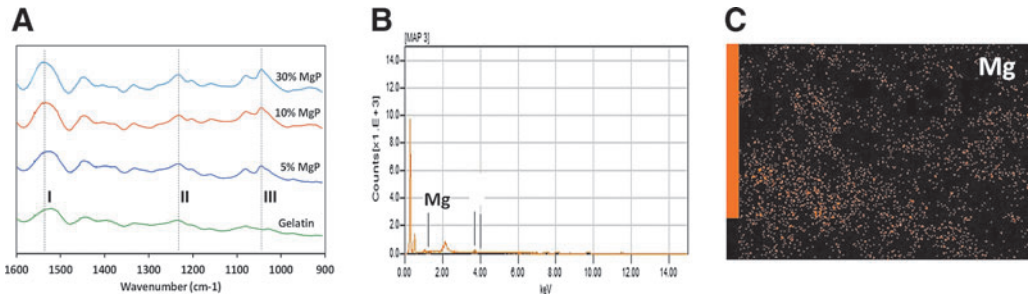

FIG. 3. **(A)** Attenuated total reflection–Fourier transform infrared (ATR-FTIR) spectra of NF-gelatin/MgP hybrid scaffolds with different amounts of MgP in the scaffolds. Dashed lines I and II assigned to gelatin, and dash line III assigned to Mg ions. **(B)** The energy dispersive X-ray spectroscopy (EDS) spectra of the NF-gelatin/MgP (MgP = 10% wt/wt) hybrid scaffold. **(C)** The EDS mappings of Mg element within the NF-gelatin/MgP (MgP = 10% wt/wt) hybrid scaffold. Color images available online at www.liebertpub.com/tea

500 nm, which is the same size range of natural collagen fibers in bone and dentin (Fig. 2C, F).[33,34]

In the ATR-FTIR spectra, the NF-gelatin/MgP scaffolds show the characteristic peaks of both the gelatin and the MgP controls, as indicated by the dashed lines in Figure 3A. Specifically, the peaks at 1542 cm^{-1} (dashed line I) and 1240 cm^{-1} (dashed line II) are assigned to the amide II (N–H bend and C–H stretch) and amide III (C–N stretch) vibrations of gelatin, respectively.[35] The band at 1055 cm^{-1} (dashed line III) is attributed to the characteristic absorption of Mg ions in the MgP,[36] and its absorption strength increased with the amount of MgP in the hybrid scaffold. The presence of MgP was further confirmed by the EDS analysis, which showed the Mg element peak in the hybrid scaffolds (Fig. 3B). In addition, the EDS mapping showed that elemental Mg was uniformly distributed on the pore walls of all of the NF-gelatin/MgP scaffolds (Fig. 3C).

The mechanical properties of the NF-gelatin/MgP scaffolds were examined and are shown in Figure 4. With a low concentration of MgP in the hybrid scaffold, the compressive modulus increased with the amount of MgP. For example, the compressive modulus of the NF-gelatin/MgP scaffold with 10% (wt/wt) MgP was 505 ± 40 kPa, which is 48.9% higher than that of the NF-gelatin control (339 ± 21 kPa). The mechanical strength of the hybrid scaffold decreased with a higher MgP concentration (> 10% wt/wt). However, the compressive modulus was still as high as 356 ± 18 kPa when the MgP concentration was 20% (wt/wt) in the hybrid scaffold.

The release of Mg ions from the hybrid scaffolds was examined and is shown in Figure 5. All the hybrid scaffolds with different MgP concentrations had similar release profiles, and a fast release rate of ~24%/day was observed for the first 3 days. For the 10% (wt/wt) MgP hybrid scaffold, it was calculated that an average of 95 ppm of Mg ions were released each day for the first 3 days. After that time, the Mg ions in the MgP of the hybrid scaffolds were released at a constant lower rate for the remaining 3 weeks. Since the NF-gelatin/MgP scaffold with 10% (wt/wt) MgP had the best mechanical strength and the desired Mg ions concentration released from the hybrid scaffold, it was used for the following cellular studies.

DPSC adhesion, proliferation, and differentiation on the hybrid scaffolds

The same number of DPSCs (5×10^5 cells/scaffold) was seeded onto both the hybrid scaffold and the NF-gelatin

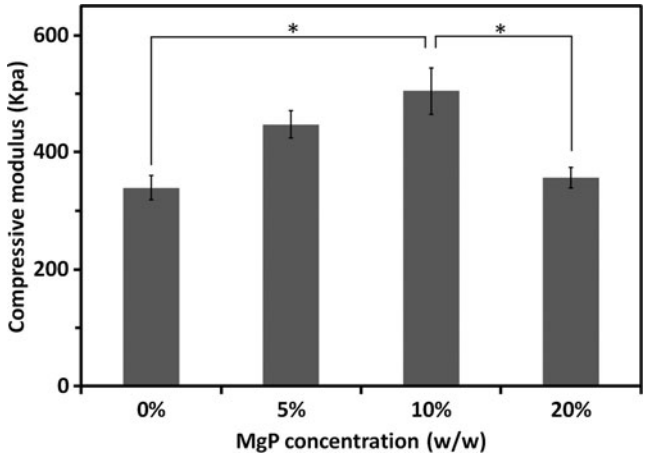

FIG. 4. Compressive moduli of the NF-gelatin/Mg hybrid scaffolds with different MgP concentrations. There was a significant difference between the NF-gelatin/MgP (MgP = 10% wt/wt) and the NF-gelatin groups (*$p < 0.05$). There was also a significant difference between the NF-gelatin/MgP (MgP = 10% wt/wt) and the NF-gelatin/MgP (MgP = 20% wt/wt) groups (*$p < 0.05$).

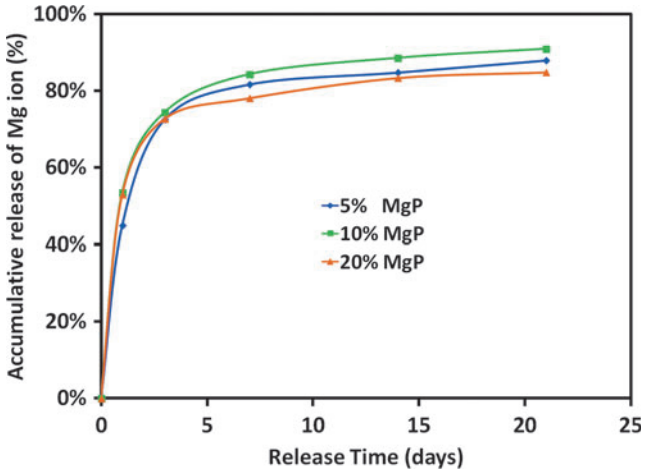

FIG. 5. Cumulative release of Mg ions from the NF-gelatin/MgP hybrid scaffolds in Tris-HCl buffer at pH 7.4 and 37°C for 3 weeks. Color images available online at www.liebertpub.com/tea

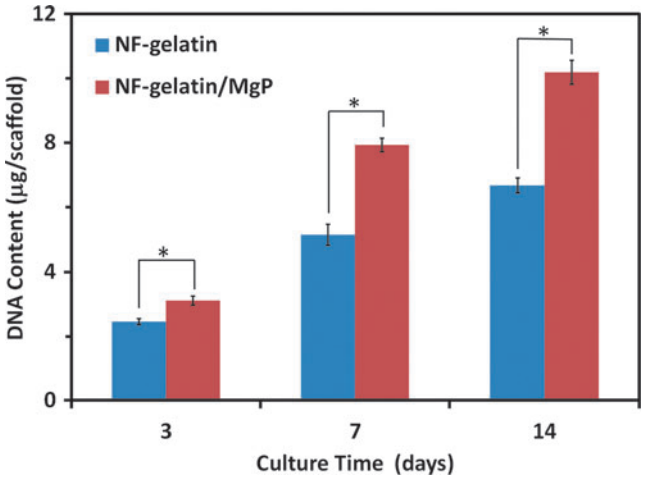

FIG. 6. The proliferation of human DPSCs cultured on NF-gelatin/MgP and NF-gelatin scaffolds. A total of 5×10^5 cells was seeded on each scaffold (*$p < 0.05$ between the NF-gelatin/MgP and the NF-gelatin groups). Color images available online at www.liebertpub.com/tea

control. During the 2-week culture period, the number of DPSCs on the NF-gelatin/MgP was always significantly higher ($p < 0.05$) than that on the NF-gelatin (Fig. 6). At 7 days, the amount of DNA on the hybrid scaffold (7.9 μg/scaffold) was more than 54.9% higher than that on the gelatin control (5.1 μg/scaffold). After 2 weeks, the DNA amount on the hybrid scaffold (10.2 μg/scaffold) was 52.2% higher than that on the control (6.7 μg/scaffold). These results indicated that the DPSCs on the NF-gelatin/MgP had a higher proliferation rate than on the NF-gelatin.

The SEM images showed the DPSCs secreted abundant ECM on both the NF-gelatin and the NF-gelatin/MgP scaffolds 2 weeks after cell seeding (Fig. 7A, B). Furthermore, the collagen fibers deposited on the NF-gelatin/MgP scaffold formed a thick matrix layer and covered the entire pore wall of the hybrid scaffold (Fig. 7B).

The ALP activity on both the hybrid and the control scaffolds increased with time for the first 3 weeks. At each time point (1, 2, and 3 weeks), the NF-gelatin/MgP group always had significantly higher ALP levels ($p < 0.05$) than did the NF-gelatin group (Fig. 7C). At 4 and 5 weeks, the ALP activity decreased for both the groups. However, the NF-gelatin/MgP group had a higher ALP expression compared to the NF-gelatin, indicating that the NF-gelatin/MgP hybrid scaffolds enhanced DPSC differentiation.

The H&E staining showed that more DPSCs penetrated into the center of the NF-gelatin/MgP scaffold than into the NF-gelatin scaffold after 5 weeks of culture in the odontogenic medium (Fig. 8A–D). Quantitative analysis indicated that 50.4% ± 2.3% and 24.6% ± 1.4% of the areas were covered with newly formed ECM in the NF-gelatin/MgP and the NF-gelatin constructs, respectively (Fig. 8E). The von Kossa staining revealed a significantly higher amount of mineral deposition in the NF-gelatin/MgP group (29.8% ± 0.9%) compared to the control group (18.7% ± 0.8%) (Fig. 8F–J).

Expressions of marker genes for odontogenic differentiation (*Col I*, *ALP*, *OCN*, *DSPP* and *DMP1*) were examined using RT-PCR, and the results are shown in Figure 9. The expression levels of all these genes were significantly higher in the NF-gelatin/MgP than in the NF-gelatin. Specifically, the expressions of *DSPP* and *Col I* on the hybrid scaffold group were more than ninefold and fourfold higher than on the control group, respectively. These results showed that the incorporation of MgP into the NF-gelatin significantly enhanced the differentiation and biomineralization of the DPSCs.

In vivo study

The specimens were retrieved after 5 weeks of subcutaneous implantation in the nude mice. The X-ray images showed that there was a considerable amount of mineral tissue formed in the NF-gelatin/MgP group, whereas there was no visible mineral tissue detected in the NF-gelatin group (Fig. 10A, B). The H&E staining images showed that the macropores in the NF-gelatin/MgP and the NF-gelatin groups were filled with newly formed dentin-like tissues (Fig. 10C–F). Quantitative measurements indicated that 77.1% ± 1.8% of the area in the NF-gelatin/MgP group was covered by the newly formed ECM, compared to 57.7% ± 3.1% of the area occupied by the newly deposited ECM in the NF-gelatin group (Fig. 10G).

To further examine the biomineralized content in the scaffolding constructs, immunohistochemistry was performed

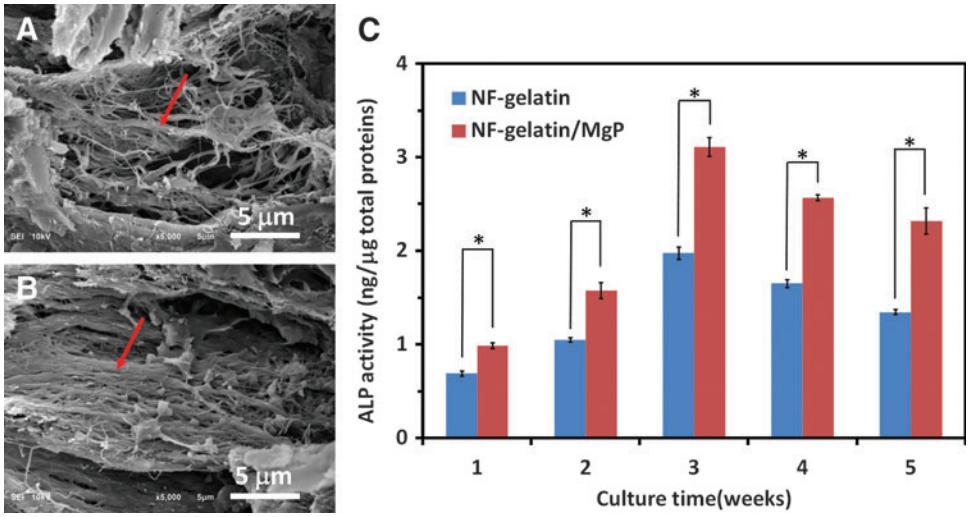

FIG. 7. **(A)** A typical SEM micrograph of human DPSCs cultured on the NF-gelatin scaffold for 3 weeks. **(B)** A typical SEM micrograph of human DPSCs cultured on the NF-gelatin/MgP scaffold for 3 weeks. More extracellular matrix was deposited on the NF-gelatin/MgP than on the NF-gelatin (red arrows). **(C)** ALP activities of human DPSCs cultured on the NF-gelatin/MgP and the NF-gelatin scaffolds for 5 weeks (*$p < 0.05$ between the NF-gelatin/MgP and the NF-gelatin groups). Color images available online at www.liebertpub.com/tea

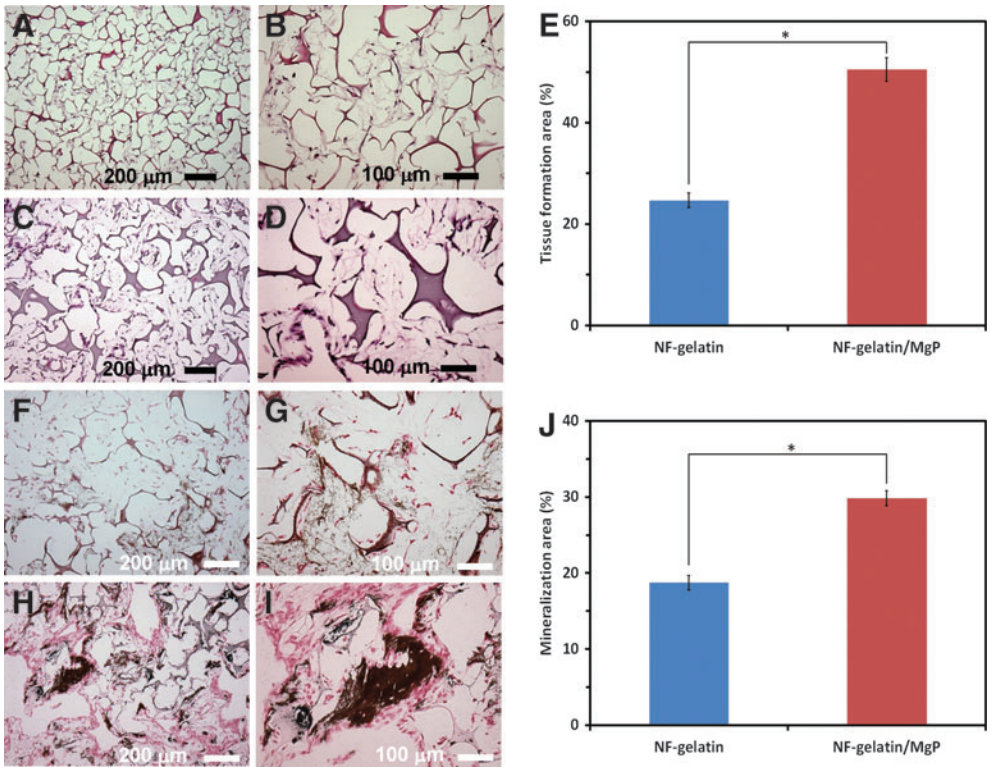

FIG. 8. Hematoxylin and eosin (H&E) and von Kossa staining images of human DPSCs cultured on NF-gelatin/MgP and NF-gelatin scaffolds for 5 weeks. **(A, B)** H&E staining of the DPSCs/NF-gelatin construct. **(C, D)** H&E staining of the DPSCs/NF-gelatin/MgP construct. **(E)** Quantitative analysis of the newly formed tissue in the DPSCs/NF-gelatin and the DPSCs/NF-gelatin/MgP constructs. **(F, G)** von Kossa staining of the DPSCs/NF-gelatin construct. **(H, I)** von Kossa staining of the DPSCs/NF-gelatin/MgP construct. **(B, D, G, I)** are high-magnification images of **(A, C, F, H),** respectively. **(J)** Quantitative analysis of the mineralized area in the DPSCs/NF-gelatin and DPSCs/NF-gelatin/MgP constructs. (*$p < 0.05$ between the NF-gelatin/MgP and the NF-gelatin group). Color images available online at www.liebertpub.com/tea

to determine the expression levels of the DSPP, DMP1, and Col I. As shown in Figure 11A–D, a strong expression (dark brown) for DSPP was detected within the pore walls of the NF-gelatin/MgP specimens, whereas much weaker staining for DSPP was visible in the NF-gelatin group. Similarly, the expression levels of DMP1 and Col I were higher in the NF-gelatin/MgP group than in the NF-gelatin group (Fig. 11E–L). All these results confirmed that more new dentin-like tissue was regenerated in the NF-gelatin/MgP scaffold than in the NF-gelatin scaffold. Because the DSPP, DMP1, and Col I antibodies used in the experiments were anti-human antibodies, these results also verified that the regenerated dental tissue came from implanted human DPSCs.

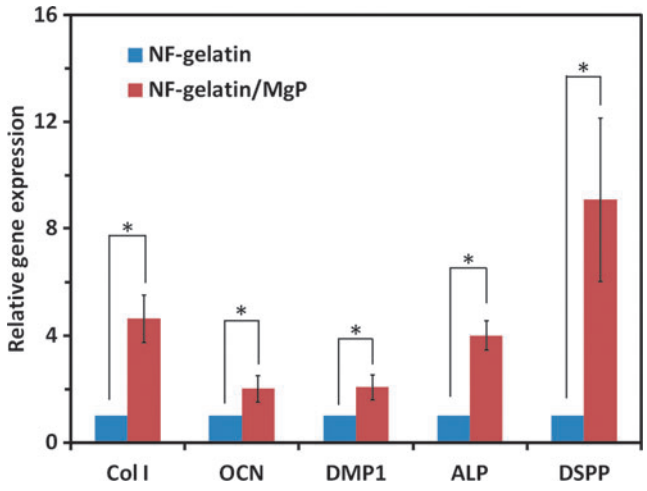

FIG. 9. Relative gene expression (*Col I*, *OCN*, *DMP1*, *ALP*, and *DSPP*) after human DPSCs were cultured on the NF-gelatin and the NF-gelatin/MgP scaffolds for 5 weeks (*$p < 0.05$ between the NF-gelatin/MgP and the NF-gelatin groups). Color images available online at www.liebertpub.com/tea

Discussion

The success of dentin tissue regeneration depends on the development of suitable scaffolding materials as carriers for dental stem/progenitor cells. Previous work by others showed that single-component scaffolding materials generated only limited dental tissues inside the scaffolding constructs,[7,15–18] suggesting that new biomimetic hybrid scaffolds must be developed to promote better dental tissue regeneration. In this study, we developed a 3D NF-gelatin/MgP hybrid scaffold that mimicked the chemical composition and nanostructured architecture of dental ECM, possessed high porosity and pore interconnectivity, and had excellent mechanical stability and sustained Mg ion release from the scaffold. The *in vitro* and *in vivo* studies showed that the integration of MgP into the hybrid scaffold significantly enhanced human DPSC proliferation, differentiation, and new dentin formation.

Introducing therapeutic ions into a scaffolding material has been considered a new approach for enhancing the bioactivity of scaffolding material.[37] Mg^{2+} is such an ion that is known to be involved in bone metabolism and plays an essential role in bone biomineralization.[38–40] Mg deficiency leads to an increased formation of osteoclasts, which results in the loss of bone mass, abnormal bone growth, and skeletal weakness.[39] Mg-doped phosphate glasses and ceramics were shown to enhance the bioactivity of the scaffolds related to osteogenesis.[22,25,41] However, to date, the effect of Mg ions on dentin regeneration is largely unknown.

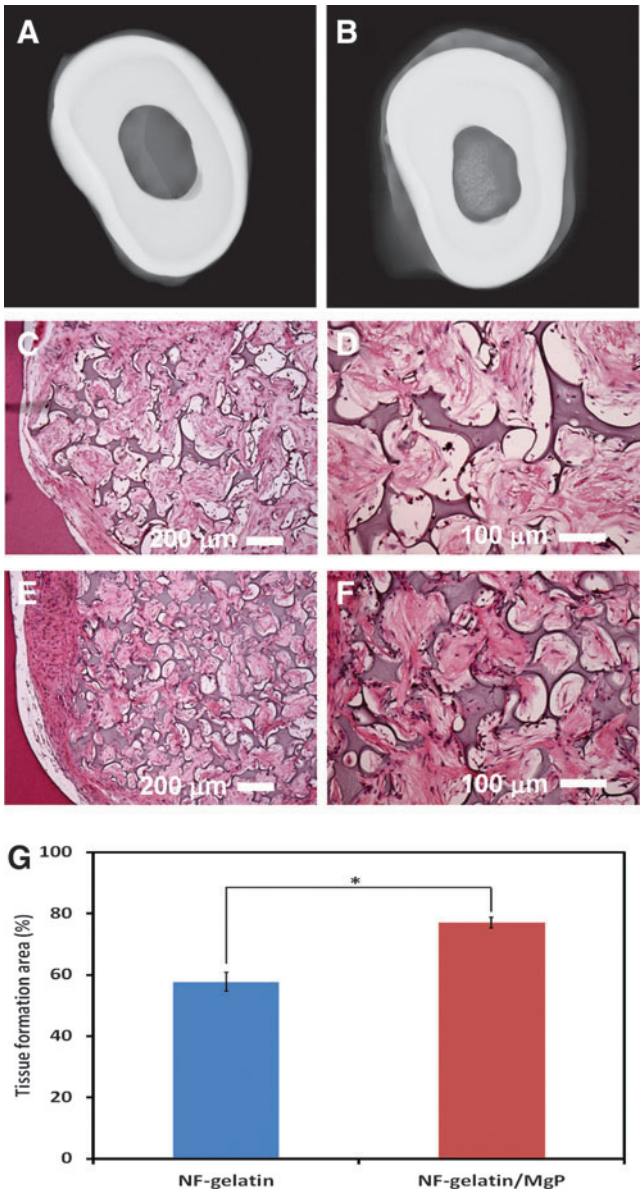

FIG. 10. X-ray and H&E staining images of human DPSCs seeded in the scaffolds with tooth slices and subcutaneously implanted in nude mice for 5 weeks. **(A)** A representative X-ray image of the NF-gelatin group showing that no minerals were detected. **(B)** A representative X-ray image of the NF-gelatin/MgP group showing a significant amount of mineral. **(C, D)** H&E staining images of the DPSCs/NF-gelatin construct. **(E, F)** H&E staining images of the DPSCs/NF-gelatin/MgP construct. **(D, F)** are the high-magnification images of **(C, E),** respectively. **(G)** Quantitative analysis of the newly formed dental tissue in the DPSCs/NF-gelatin and the DPSCs/NF-gelatin/MgP constructs. (*$p < 0.05$ between the NF-gelatin/MgP and the NF-gelatin group). Color images available online at www.liebertpub.com/tea

Because dentin closely resembles bone physically and chemically, we hypothesized that the incorporation of Mg into our nanostructured gelatin scaffolds will accelerate dentin tissue formation. We tested our hypothesis first in 2D cell culture plates and found that the addition of Mg ions (up to 1000 ppm) into the culture medium significantly enhanced DPSC differentiation and biomineralization (Fig. 1B, C). Similar results were observed when Mg ions were added to treat human embryonic stem cells.[42] The accelerated differentiation and biomineralization from the addition of Mg ions is believed to be attributed to the activation of ALP and promotion of crystallization processes and pattern formation of the inorganic mineral phase.[20,23] Several studies reported that proliferating cells had more Mg than did nonproliferating cells and that the Mg inside the cells stimulates protein and DNA synthesis.[43–46] However, only the addition of low Mg ion concentration ($\leq$100ppm) promoted both the proliferation and differentiation of the DPSCs (Fig. 1A). A high amount of Mg ions ($\geq$500 ppm) in the culture medium might interfere with the ion balance in the plasma membrane, leading to cytotoxicity and therefore inhibiting cellular proliferation. Because of that, we chose the release of low Mg ion concentration ($\sim$100 ppm) from the 3D NF-gelatin/MgP hybrid scaffolds for the next cellular experiments.

Directly mixing biodegradable polymer substrates with inorganic particles is a simple approach to synthesizing hybrid scaffolds. Several gelatin-based hybrid scaffolds have been developed using this method.[47–49] However, directly mixing inorganic particles with polymer solution generally forms a heterogeneous mixture that results in an uneven distribution of the composition within the composite, as well as limited mechanical strength. In the present study, we used a homogenous solution composed of gelatin and the MgP precursor solution to prepare the NF-gelatin/MgP hybrid scaffolds. The MgP was synthesized by the reaction of magnesium oxide with calcium dihydrogen phosphate during the solvent cast and TIPS process. After porogen leaching and crosslinking of the gelatin matrix, a nanofibrous composite scaffold with uniform distribution of MgP throughout the hybrid was obtained and confirmed by the EDS measurement (Fig. 3C). The mechanical strength of the NF-gelatin/MgP hybrid scaffold (MgP = 10% wt/wt) was also significantly higher ($p < 0.05$) than that of the NF-gelatin (Fig. 4). A high amount of MgP (MgP = 20% wt/wt) in the hybrid scaffold did not contribute to the overall mechanical properties, probably due to its interference with the phase separation of the gelatin solution during the scaffold formation.

When NF-gelatin/MgP scaffolds contact aqueous solution, the hydrophilic gelatin nanofibers absorb water and expand; therefore, the Mg ions from the MgP will be released from the hybrid scaffold (Fig. 5). For the NF-gelatin/MgP hybrid scaffold with 10% MgP, the average amount of released Mg ions each day for the first 3 days was 95 ppm, which is in the concentration range that enhances both the proliferation and differentiation of DPSCs (Fig. 1). After 3 days, the remaining MgP was released at a constant, lower rate for more than 3 weeks. To achieve a sustained release of Mg at a constant concentration from the NF-gelatin/MgP hybrid scaffold for a longer time, an optimized MgP composition and scaffolding preparation condition will be needed in a future work.

In the NF-gelatin/MgP hybrid scaffold, the NF-gelatin scaffold mimicked the collagen of the dentin matrix (physically and chemically) and possessed high surface area, porosity, pore interconnectivity, and had excellent mechanical stability. The controlled release of Mg ions from the MgP further provided desirable chemical signals to enhance the DPSC proliferation and differentiation. Therefore,

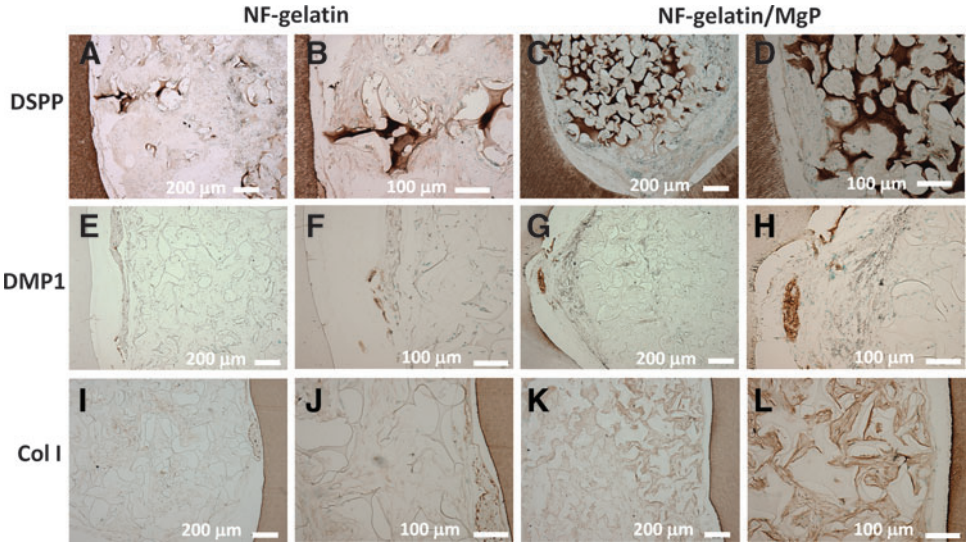

FIG. 11. Immunohistochemical staining imagines of odontogenesis markers for DPSCs/NF-gelatin and the DPSCs/NF-gelatin/MgP constructs after being subcutaneously implanted in nude mice for 5 weeks. **(A, B)** DSPP expression on the DPSCs/NF-gelatin construct. **(C, D)** DSPP expression on the DPSCs/NF-gelatin/MgP construct. **(E, F)** DMP1 expression on the DPSCs/NF-gelatin construct. **(G, H)** DMP1 expression on the DPSCs/NF-gelatin/MgP construct. **(I, J)** Col I expression on the DPSCs/NF-gelatin construct. **(K, L)** Col I expression on the DPSCs/NF-gelatin/MgP construct. **(B, D, F, H, J, L)** are the high-magnification images of **(A, C, E, G, I, K)**, respectively. Color images available online at www.liebertpub.com/tea

the hybrid NF-gelatin/MgP creates a better microenvironment to facilitate DPSC/material interactions in the scaffolds. These *in vitro* studies indicated that the DPSCs in the hybrid scaffold had a significantly higher proliferation rate than in the NF-gelatin control under the same culture conditions (Fig. 6). Furthermore, the NF-gelatin/MgP group had a higher ALP expression, greater ECM deposition, and stronger von Kossa staining than did the NF-gelatin group in the same differentiation medium (Figs. 7 and 8). The expression levels of the marker genes for odontogenic differentiation (*Col I*, *ALP*, *OCN*, *DSPP*, and *DMP1*) were all significantly higher in the NF-gelatin/MgP than in the NF-gelatin, confirming that the incorporation of MgP into NF-gelatin enhanced the differentiation of the DPSCs (Fig. 9). Consistently, we observed more hard tissue formation and more dentin-like matrix deposition in the NF-gelatin/MgP group than in the NF-gelatin group when the DPSC/scaffold constructs were subcutaneously implanted *in vivo* for 5 weeks (Fig. 10). Strong positive immunohistochemical staining for DSPP, DMP1, and Col1 in the NF-gelatin/MgP group also confirmed the differentiation of the DPSCs to odontoblast cells. Thus, our NF-gelatin/MgP was an excellent cell carrier to facilitate DPSC differentiation and to form dense and mineralized dentin-like tissue. However, the tissue formed in the scaffold was not the typical well-organized tubular dentin; further investigation to optimize the scaffold architecture and identify other chemical/biological cues is necessary to facilitate more natural dentin tissue formation.

Conclusions

Biomimetic nanostructured NF-gelatin/MgP scaffolds were prepared in this study. The hybrid scaffold not only physically and chemically mimicked the dentin matrix but also provided sustained Mg ion release from the matrix, thus creating favorable physical and chemical cues to guide dental stem/progenitor cell growth and differentiation in the scaffold. The *in vitro* and *in vivo* studies showed that the NF-gelatin/MgP hybrid scaffold significantly enhanced human DPSC proliferation, differentiation, and new dentin formation compared to the NF-gelatin control. The biomimetic NF-gelatin/MgP hybrid scaffolds, therefore, are promising candidates for dental tissue regeneration.

Acknowledgments

The authors are grateful to Dr. Songtao Shi, University of Southern California, for kindly providing the human DPSCs. This study was supported by NIH/NIDCR 1R03DE22838-01A1 and Texas A&M—Weizmann Collaborative Program to X.L., and the National Natural Science Foundation of China (no. 31200738) to T.Q. We thank Jeanne Santa Cruz for her assistance with the editing of this article.

Disclosure Statement

No competing financial interests exist.

References

1. Selwitz, R.H., Ismail, A.I., and Pitts, N.B. Dental caries. Lancet **369,** 51, 2007.
2. Dental Caries (Tooth decay) www.nidcr.nih.gov/DataStatistics/FindDataByTopic/DentalCaries/ (accessed November 13, 2013).
3. Gerritsen, A.E., Allen, P.F., Witter, D.J., Bronkhorst, E.M., and Creugers, N.H. Tooth loss and oral health-related quality of life: a systematic review and meta-analysis. Health Qual Life Outcomes **8,** 126, 2010.
4. Noble, J.M., Scarmeas, N., and Papapanou, P.N. Poor oral health as a chronic, potentially modifiable dementia risk factor: review of the literature. Curr Neurol Neurosci Rep **13,** 1, 2013.

5. Reeh, E.S., Messer, H.H., and Douglas, W.H. Reduction in tooth stiffness as a results of endodontic and restorative procedures. J Endodont **15,** 512, 1989.
6. Modino, S.A., and Sharpe, P.T. Tissue engineering of teeth using adult stem cells. Arch Oral Biol **50,** 255, 2005.
7. Galler, K.M., Cavender, A., Yuwono, V., Dong, H., Shi, S.T., Schmalz, G., *et al.* Self-assembling peptide amphiphile nanofibers as a scaffold for dental stem cells. Tissue Eng Part A **14,** 2051, 2008.
8. Nakashima, M., and Akamine, A. The application of tissue engineering to regeneration of pulp and dentin in endodontics. J Endodont **31,** 711, 2005.
9. Gronthos, S., Mankani, M., Brahim, J., Robey, P.G., and Shi, S. Postnatal human dental pulp stem cells (DPSCs) *in vitro* and *in vivo*. Proc Natl Acad Sci U S A **97,** 13625, 2000.
10. Karageorgiou, V., and Kaplan, D. Porosity of 3D biomaterial scaffolds and osteogenesis. Biomaterials **26,** 5474, 2005.
11. Liu, X., and Ma, P.X. Polymeric scaffolds for bone tissue engineering. Ann Biomed Eng **32,** 477, 2004.
12. Liu, X., Won, Y., and Ma, P.X. Surface modification of interconnected porous scaffolds. J Biomed Mater Res Part A **74,** 84, 2005.
13. Liu, X., Smith, L.A., Hu, J., and Ma, P.X. Biomimetic nanofibrous gelatin/apatite composite scaffolds for bone tissue engineering. Biomaterials **30,** 2252, 2009.
14. Sun, Y., Jiang, Y., Liu, Q.J., Gao, T., Feng, J.Q., Dechow, P., *et al.* Biomimetic engineering of nanofibrous gelatin scaffolds with noncollagenous proteins for enhanced bone regeneration. Tissue Eng Part A **19,** 1754, 2013.
15. Zhang, W., Frank Walboomers, X., van Kuppevelt, T.H., Daamen, W.F., Bian, Z., and Jansen, J.A. The performance of human dental pulp stem cells on different three-dimensional scaffold materials. Biomaterials **27,** 5658, 2006.
16. Huang, G.T.-J., Yamaza, T., Shea, L.D., Djouad, F., Kuhn, N.Z., Tuan, R.S., *et al.* Stem/progenitor cell–mediated *de novo* regeneration of dental pulp with newly deposited continuous layer of dentin in an *in vivo* model. Tissue Eng Part A **16,** 605, 2009.
17. Wang, J., Liu, X., Jin, X., Ma, H., Hu, J., Ni, L., *et al.* The odontogenic differentiation of human dental pulp stem cells on nanofibrous poly (l-lactic acid) scaffolds *in vitro* and *in vivo*. Acta Biomater **6,** 3856, 2010.
18. Prescott, R.S., Alsanea, R., Tayad, M.I., Johnson, B.R., Wenckus, C.S., Hao, J., *et al. In vivo* generation of dental pulp-like tissue by using dental pulp stem cells, dentin matrix protein 1 transplantation in mice. J Endodont **34,** 421, 2008.
19. Wiesmann, H.P., Tkotz, T., Joos, U., Zierold, K., Stratmann, U., Szuwart, T., *et al.* Magnesium in newly formed dentin mineral of rat incisor. J Bone Miner Res **12,** 380, 1997.
20. Saris, N.E.L., Mervaala, E., Karppanen, H., Khawaja, J.A., and Lewenstam, A. Magnesium—an update on physiological, clinical and analytical aspects. Clin Chim Acta **294,** 1, 2000.
21. Serre, C.M., Papillard, M., Chavassieux, P., Voegel, J.C., and Boivin, G. Influence of magnesium substitution on a collagen-apatite biomaterial on the production of a calcifying matrix by human osteoblasts. J Biomed Mater Res **42,** 626, 1998.
22. Staiger, M.P., Pietak, A.M., Huadmai, J., and Dias, G. Magnesium and its alloys as orthopedic biomaterials: a review. Biomaterials **27,** 1728, 2006.
23. Bigi, A., Foresti, E., Gregorini, R., Ripamonti, A., Roveri, N., and Shah, J.S. The role of magnesium on the structure of biological apatites. Calcif Tissue Int **50,** 439, 1992.
24. Sun, H.L., Wu, C.T., Dai, K.R., Chang, J., and Tang, T.T. Proliferation and osteoblastic differentiation of human bone marrow-derived stromal cells on akermanite-bioactive ceramics. Biomaterials **27,** 5651, 2006.
25. Hussain, A., Bessho, K., Takahashi, K., and Tabata, Y. Magnesium calcium phosphate as a novel component enhances mechanical/physical properties of gelatin scaffold and osteogenic differentiation of bone marrow mesenchymal stem cells. Tissue Eng Part A **18,** 768, 2012.
26. Wei, J., Jia, J.F., Wu, F., Wei, S.C., Zhou, H.J., Zhang, H.B., *et al.* Hierarchically microporous/macroporous scaffold of magnesium-calcium phosphate for bone tissue regeneration. Biomaterials **31,** 1260, 2010.
27. Kim, B.S., Kim, J.S., Park, Y.M., Choi, B.Y., and Lee, J. Mg ion implantation on SLA-treated titanium surface and its effects on the behavior of mesenchymal stem cell. Mater Sci Eng C Mater Biol Appl **33,** 1554, 2013.
28. Liu, X.H., and Ma, P.X. Phase separation, pore structure, and properties of nanofibrous gelatin scaffolds. Biomaterials **30,** 4094, 2009.
29. Jia, J., Zhou, H., Wei, J., Jiang, X., Hua, H., Chen, F., *et al.* Development of magnesium calcium phosphate biocement for bone regeneration. J R Soc Interface **7,** 1171, 2010.
30. Qu, T.J., and Liu, X.H. Nano-structured gelatin/bioactive glass hybrid scaffolds for the enhancement of odontogenic differentiation of human dental pulp stem cells. J Mater Chem B **1,** 4764, 2013.
31. Nair, A., Shen, J., Lotfi, P., Ko, C.Y., Zhang, C.C., and Tang, L. Biomaterial implants mediate autologous stem cell recruitment in mice. Acta Biomater **7,** 3887, 2011.
32. Galler, K., Schweikl, H., Hiller, K.-A., Cavender, A., Bolay, C., D'Souza, R., *et al.* TEGDMA reduces mineralization in dental pulp cells. J Dent Res **90,** 257, 2011.
33. Termine, J.D., Belcourt, A.B., Conn, K.M., and Kleinman, H. Mineral and collagen-binding proteins of fetal calf bone. J Biol Chem **256,** 10403, 1981.
34. Habelitz, S., Balooch, M., Marshall, S.J., Balooch, G., and Marshall, G.W. *In situ* atomic force microscopy of partially demineralized human dentin collagen fibrils. J Struct Biol **138,** 227, 2002.
35. Sisson, K., Zhang, C., Farach-Carson, M.C., Chase, D.B., and Rabolt, J.F. Evaluation of cross-linking methods for electrospun gelatin on cell growth and viability. Biomacromolecules **10,** 1675, 2009.
36. Miller, F.A., and Wilkins, C.H. Infrared spectra and characteristic frequencies of inorganic ions—their use in quanlitative analysis. Anal Chem **24,** 1253, 1952.
37. Hoppe, A., Guldal, N.S., and Boccaccini, A.R. A review of the biological response to ionic dissolution products from bioactive glasses and glass-ceramics. Biomaterials **32,** 2757, 2011.
38. Rude, R.K., Gruber, H.E., Norton, H.J., Wei, L.Y., Frausto, A., and Kilburn, J. Dietary magnesium reduction to 25% of nutrient requirement disrupts bone and mineral metabolism in the rat. Bone **37,** 211, 2005.
39. Belluci, M.M., Schoenmaker, T., Rossa, C., Orrico, S.R., de Vries, T.J., and Everts, V. Magnesium deficiency results in an increased formation of osteoclasts. J Nutr Biochem **24,** 1488, 2013.
40. Rude, R.K., Gruber, H.E., Norton, H.J., Wei, L.Y., Frausto, A., and Kilburn, J. Reduction of dietary magnesium by only

50% in the rat disrupts bone and mineral metabolism. Osteoporosis Int **17,** 1022, 2006.
41. Witte, F., Feyerabend, F., Maier, P., Fischer, J., Stoermer, M., Blawert, C., *et al.* Biodegradable magnesium-hydroxyapatite metal matrix composites. Biomaterials **28,** 2163, 2007.
42. Nguyen, T.Y., Garcia, S., Liew, C.G., and Liu, H. Effects of magnesium on growth and proliferation of human embryonic stem cells. Conf Proc IEEE Eng Med Biol Soc **2012,** 723, 2012.
43. Cameron, I.L., and Smith, N.K.R. Cellular concentration of magnesium and other ions in relation to protein-synthesis, cell proliferation and cancer. Magnesium **8,** 31, 1989.
44. Nasulewicz, A., Wietrzyk, J., Wolf, F.I., Dzimira, S., Madej, J., Maier, J.A.M., *et al.* Magnesium deficiency inhibits primary tumor growth but favors metastasis in mice. Biochim Biophys Acta Mol Basis Dis **1739,** 26, 2004.
45. Wolf, F.I., Fasanella, S., Tedesco, B., Torsello, A., Sgambato, A., Faraglia, B., *et al.* Regulation of magnesium content during proliferation of mammary epithelial cells (HC-11). Front Biosci **9,** 2056, 2004.
46. Gunther, T. Concentration, compartmentation and metabolic function of intracellular free Mg2+. Magnes Res **19,** 225, 2006.
47. Kim, H.W., Song, J.H., and Kim, H.E. Nanoriber generation of gelatin-hydroxyapatite biomimetics for guided tissue regeneration. Adv Funct Mater **15,** 1988, 2005.
48. Wang, M.B., Li, Y.B., Wu, J.Q., Xu, F.L., Zuo, Y., and Jansen, J.A. *In vitro* and *in vivo* study to the biocompatibility and biodegradation of hydroxyapatite/poly(vinyl alcohol)/gelatin composite. J Biomed Mater Res Part A **85A,** 418, 2008.
49. Zhao, F., Yin, Y.J., Lu, W.W., Leong, J.C., Zhang, W.J., Zhang, J.Y., *et al.* Preparation and histological evaluation of biomimetic three-dimensional hydroxyapatite/chitosan-gelatin network composite scaffolds. Biomaterials **23,** 3227, 2002.

Address correspondence to:
Xiaohua Liu, PhD
Department of Biomedical Sciences
Texas A&M University Baylor College of Dentistry
3302 Gaston Ave.
Dallas, TX 75246

E-mail: xliu@bcd.tamhsc.edu

Received: December 5, 2013
Accepted: February 14, 2014
Online Publication Date: April 2, 2014